Optimal placement of magnets in Indus-2 storage ring

Riyasat Husain[1)] A D Ghodke Gurnam Singh
Raja Ramanna Centre for Advanced Technology, Indore 452013, India

Abstract: In Indus-2, by optimizing the position of the magnetic elements, using the simulated annealing algorithm, at different locations in the ring with their field errors, the effects on beam parameters have been minimized. Closed orbit distortion and beta beat are considerably reduced by optimizing the dipole and quadrupole magnets positions in the ring. For the Indus-2 storage ring, sextupole optimization gives insignificant improvement in dynamic aperture with chromaticity-correcting sextupoles. The magnets have been placed in the ring with the optimized sequence and storage of the beam has been achieved at injection energy without energizing any corrector magnets. Magnet sorting has led to the easy beam current accumulation and the measurement of parameters such as closed orbit distortion, beta function, dispersion, dynamic aperture etc.

Key words: sorting, magnet-to-magnet errors, beta beat, closed orbit distortion, dynamic aperture, simulated annealing

PACS: 29.20.D-, 29.25.Bx, 02.60.Pn **DOI:** 10.1088/1674-1137/39/3/037002

1 Introduction

Indus-2 [1], a 2.5 GeV electron storage ring, is now operational at the Raja Ramanna Centre for Advanced Technology, Indore, India. This is the second electron storage ring after Indus-1, a 0.45 GeV electron storage ring. Both the sources share a common injector system consisting of a 20 MeV microtron and a 0.45–0.70 GeV synchrotron. In Indus-2 the beam injection takes place at 0.55 GeV and the beam energy is further ramped to 2.5 GeV to provide the beam to the synchrotron light users for the experiments. The Indus-2 ring lattice consists of 8 unit cells of a double bend achromat or expanded Chasman Green lattice. Each unit cell accommodates 2 dipoles, 9 quadrupoles and 4 sextupoles. The ring consists of a total of 16 dipoles, 72 quadrupoles grouped in five families: Q1D (16), Q2F (16), Q3D (16), Q4F (16) & Q5D (8) and 32 sextupoles grouped in two families SF (16) and SD (16). All 16 dipoles are connected in series and driven by a single power supply. A pair of quadrupoles in the first three families is driven in series by one power supply and therefore there are 24 power supplies for 48 quadrupoles in these three families. There is one power supply for Q4F and one power supply for the Q5D family of quadrupoles. Thus 72 quadrupoles are powered by a total of 26 power supplies. There are 2 power supplies for the sextupoles, one for SF and another for the SD family. In addition there are 48 horizontal and 40 vertical corrector magnets driven by independent power supplies for the correction of closed orbit distortion (COD). The lattice functions of one unit cell with a magnetic structure are shown in Fig. 1. In Table 1, the strengths of the magnets for the design tune (9.3, 5.2) and chromaticity (2, 2) are listed together with their numbers and the number of power supplies driving the magnets. Table 2 lists some of the design parameters of the Indus-2 storage ring. The storage ring has tight tolerances for magnetic field and alignment errors to achieve the desired performance. In

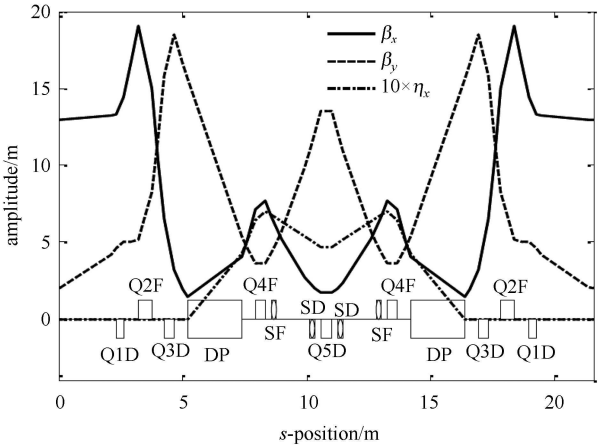

Fig. 1. Lattice functions and arrangement of the magnetic elements in one unit cell of Indus-2. Shown with the rectangles are DP-dipole magnets; Q1D, Q3D & Q5D- defocusing quadrupoles; Q2F & Q4F focusing quadrupoles and SF & SD-focusing & defocusing sextupole magnets.

Received 26 February 2014, Revised 27 October 2014

1) E-mail: riyasat@rrcat.ernet.in

Table 1. Strength of the magnets for tune (9.3, 5.2) and corrected chromaticity (2, 2).

name of family	type of magnets	length/m	normalized strength	No. of magnets	No. of power supplies
DP	dipole	2.1795	0.3927 rad	16	1
Q1D	quadrupole	0.30	-0.7986 m^{-2}	16	8
Q2F	quadrupole	0.55	1.5377 m^{-2}	16	8
Q3D	quadrupole	0.40	-1.6938 m^{-2}	16	8
Q4F	quadrupole	0.40	1.8197 m^{-2}	16	1
Q5D	quadrupole	0.40	-1.1165 m^{-2}	8	1
SF	sextupole	0.20	12.51 m^{-3}	16	1
SD	sextupole	0.20	-11.52 m^{-3}	16	1

every fabricated magnet, for a given excitation current, there is normally a deviation of the field from its design value. There are large numbers of magnets and the magnet-to-magnet field deviations are present and their disturbing effects are unavoidable. These disturbing effects on the beam can be minimized if the field deviations are known from the magnet measurements and the places of the magnets are optimized with some well-defined procedures. In this paper, we report the method to optimize the magnetic element locations and benefits which are achieved by placing them as per this procedure in the ring. With this optimal sequence of the placement of the magnetic elements, the electron beam circulated first one turn and later four turns with injection kickers off. With injection kickers turned on beam circulation lasted for ∼2.5 ms (1 turn is equal to ∼575 ns revolution time) and later with RF cavity turned on the storage of electron beam without energizing any of the steering magnets has been achieved. Presently Indus-2 is operated at full energy of 2.5 GeV with 100 mA beam current in user mode.

Table 2. A few design parameters of Indus-2 storage ring.

parameters	values
energy/GeV	0.55–2.5
beam current/mA	300
circumference/m	172.4743
betatron tunes	9.3/5.2
natural chromaticities	$-19/-12$
beam emittance/(nm·rad)	58
momentum compaction factor	5.1e-3
equilibrium energy spread	8.9e-4
RF frequency/MHz	505.8
harmonic number	291

Since the beam injection and accumulation is the most critical part of the storage ring, the magnetic sorting was performed at injection energy. The paper is divided in sections as follows: in Section 2, we discuss the effects of the magnetic field errors on beam parameters and the objective functions which are to be minimized. In Section 3, we describe the optimization algorithms. The simulation results for the sorting of magnets are presented and discussed in Section 4. The measurement of COD, beam accumulation rate, beta beat and dynamic aperture etc. are discussed in Section 5.

2 Objective functions

The objective or cost function is a measure of the goodness of a particular configuration of parameters. The selection of an appropriate cost function is crucial for achieving good results. The objective functions which are affected by the field errors are defined independently for each type of magnet [2]. The optimization procedure based on the simulated annealing algorithm [2–5] is applied for the sorting of dipoles, quadrupoles and sextupoles. The error in the field strength of the individual magnet is defined as the deviation of its integrated field strength from the average value of the field strength. Let k be the field error which is considered as a kick at the centre of the magnet. An array of the error set is built up in a specific sequence, $\underline{d}=(k_1, k_2, \cdots, k_i, \cdots, k_M)$ depending on their positions in the ring, where M denotes the M^{th} magnet. The objective function W is constructed and is used for comparison with the objective function obtained with a different permutation of the error set. The objective function (W) is taken as the root mean square of W_i defined by $W_i=\sqrt{A_i^2+B_i^2}$ where A_i and B_i at i^{th} observation point are constructed for each type of magnet errors independently. It can be shown that at the point of kick, only the A-component gets affected and between the kicks vector W is simply rotated with an appropriate phase advance, changing A and B but preserving its length [6]. Because of this invariant character of W one observation point per kick is sufficient. By permutation of the errors a new objective function is constructed and used to optimize the disturbing effects. In the following subsections the objective functions for each type of magnet are discussed.

2.1 Dipole magnets

It is known that the dipole errors give rise to closed orbit distortion. In order to minimize this distortion we define the objective function required by the optimization method. Let the error strength in the i^{th} magnet

be k_i=θ_i−θ_0, where θ_i and θ_0 are measured and the design values of the normalized integrated field strengths of the $i^{\rm th}$ dipole magnet. The error strength k_i is given in terms of measured magnet-to-magnet field errors by $k_i = (\Delta BL/\langle BL\rangle)_i\theta_0$, where $\langle BL\rangle$ is the average integrated strength of the dipole magnets.

To obtain the physical (stable) solution, the orbit kicked by the error k must oscillate in a closed loop around the ring. A single kick k and disturbed closed orbit vector (x, x') are related by the one turn transfer matrix of the ring

$$\begin{pmatrix} x \\ x' \end{pmatrix} = M_{\rm rev}\begin{pmatrix} x \\ x' \end{pmatrix} + \begin{pmatrix} 0 \\ k \end{pmatrix}. \tag{1}$$

The amplitude of the closed orbit is given by

$$x = \frac{k\sqrt{\beta\beta_i}\cos(|\mu-\mu_i|-\phi/2)}{2\sin(\phi/2)}, \tag{2}$$

where β and β_i are the beta functions at the observation point and the kick point respectively, $\Delta\mu$=$|\mu-\mu_i|$, is the phase difference between the kick position and the point of observation.

Several kicks at different locations are added by linear superposition to get the resulting closed orbit (x_i, x_i') at the $i^{\rm th}$ observation point. The vector (A,B) is constructed by using the local twiss parameters (α_i, β_i) at that observation point. The components of vector (A, B) are defined as [2, 6]

$$A_i = \frac{\alpha_i x_i+\beta_i x_i'}{\sqrt{\beta_i}}, \quad B_i = \frac{x_i}{\sqrt{\beta_i}}. \tag{3}$$

These are used to construct a component W_i at this observation point. This is equivalent to the Courant Snyder invariant of the closed orbit distortion. The objective function is the root mean square of all W_i calculated at all the observation points in the ring. Minimizing this function for dipoles will reduce the amplitudes and slopes of the closed orbit oscillations over the ring.

2.2 Quadrupole magnets

The quadrupole field gradient errors lead to beta beat and change the in tune value of the machine. The quadrupole gradient error $k_i = K_i - K_0$, between the measured and design-integrated normalized quadrupole strength is assumed to be located as a kick at the centre of the quadrupole. In terms of relative field errors ($\Delta GL/\langle GL\rangle$) the error k is defined by k = $(\Delta GL/\langle GL\rangle)K_0$, where K_0 is the normalized quadrupole strength. Here G is the quadrupole field gradient and L is the length of the magnet. These errors generate, in general, the distortion in the twiss parameter $\Delta\beta$ and is given by [2, 6]

$$\frac{\Delta\beta}{\beta_0} = -\beta k\frac{\cos(|\mu-\mu_i|-\phi)}{2\sin\phi}. \tag{4}$$

The components of vector (A, B) for this case are constructed by

$$A_i = \frac{\alpha_i\beta_{0i}-\beta_i\alpha_{0i}}{\sqrt{\beta_i\beta_{0i}}}, \quad B_i = \frac{\beta_i-\beta_{0i}}{\sqrt{\beta_i\beta_{0i}}}. \tag{5}$$

Here (α_0, β_0) and (α, β) are the twiss parameters corresponding to the design strength and the error added strength at the point of observation respectively. The objective function W is defined as the rms value of the vectors (A, B) constructed in horizontal and vertical planes. Minimizing this type of objective function will, in effect, reduce the beta beating.

2.3 Sextupole magnets

We have considered five distortion functions defined by T. Collins [2, 6]. These distortion functions describe the nonlinear effects of sextupoles which are denoted by (A_1, B_1), (A_3, B_3), ($A_{\rm s}$, $B_{\rm s}$), ($A_{\rm d}$, $B_{\rm d}$) and ($\underline{A}$, $\underline{B}$), where A_m functions are the derivatives of B_m functions. These functions incorporate the effect of the resonances driven by sextupoles and are defined by

$$B_m = s_m\frac{\cos(|\Delta\psi_m|-\phi_m/2)}{8\sin(\phi_m/2)}, \tag{6}$$

with $A_m = B_m'$, where the sextupole strength is normalized as

$$s_m = \sqrt{\frac{\beta_x^3}{\beta_0}}S, \tag{7}$$

where S is the sextupole strength normalized with the beam energy.

The following is the procedure to construct the objective function for sextupole sorting: calculate functions (A_{m0}, B_{m0}) using sextupole at their design field strengths and (A_m, B_m) including the field errors. The difference (A_m-A_{m0}, B_m-B_{m0}) is now the vector (A, B). The rms of all five vectors constructs the objective function. Minimizing these functions by sextupole locations optimization with their field errors reduces the nonlinear beam mismatch and improves the dynamic aperture.

We have also used another objective function which describes the beam envelope smear [7, 8] as

$$\begin{aligned} A_{xi} = {} & \frac{\sqrt{\beta_{xi}}}{8}\sum_j\sqrt{\beta_{xj}}S_j\Bigg\{(J_x\beta_{xj}-2J_y\beta_{yj}) \\ & \times\frac{\cos(-\pi\nu_x+|\mu_{xij}|)}{\sin(\pi\nu_x)}+J_x\beta_{xj}\frac{\cos3(-\pi\nu_x+|\mu_{xij}|)}{\sin(3\pi\nu_x)} \\ & -J_y\beta_{yj}\frac{\cos[-\pi(\nu_x+2\nu_y)+2|\mu_{yij}|]}{\sin\pi(\nu_x+2\nu_y)} \\ & -J_y\beta_{yj}\frac{\cos[-\pi(\nu_x-2\nu_y)-2|\mu_{yij}|]}{\sin\pi(\nu_x-2\nu_y)}\Bigg\}, \end{aligned} \tag{8}$$

$$B_{yi} = -\frac{\sqrt{J_x J_y \beta_{yi}}}{8}\sum_j \sqrt{\beta_{xj}\beta_{yj}}S_j \times\left\{\frac{\cos[-\pi(\nu_x+2\nu_y)+|\mu_{xij}+2\mu_{yij}|]}{\sin\pi(\nu_x+2\nu_y)} -\frac{\cos[-\pi(\nu_x-2\nu_y)+|\mu_{xij}-2\mu_{yij}|]}{\sin\pi(\nu_x-2\nu_y)}\right\}. \quad (9)$$

The indices i and j denote the point of observation and location of the sextupole magnets and $J_{x,y}$ is the action variable equal to half of the emittance in the horizental and vertical plane respectively. Minimizing these kinds of functions by sextupole locations with their field errors will improve the dynamic aperture and reduce the amplitude-dependent tune shift.

3 Optimization algorithm: simulated annealing [2–5]

There are many schemes to optimize the locations of the magnets in the lattice based on their field errors. The simplest is the local compensation in which magnets are placed along the beam direction of the accelerator based on the pairing of the magnets with similar errors, which are mutually compensated by an appropriate phase advance in the lattice. Generally, this method does not work for the cases where the required phase relationship between the error locations is not met in the lattice. Another method one can think of is to permute all the magnets and for all the permutations check for the global minimum of the objective function. But for a large number of magnets, all such possible permutations grow exponentially. A computer simulation to check all possible permutations would be too time-consuming. The method of simulated annealing is typically applied for these kinds of problems to find a solution close to the global minimum in a reasonable time limit. For a given set of error vectors, the value of the objective function W_0 is calculated and compared with the objective function obtained with a permutated error set. The new permutation is obtained from the previous one by a few well-defined steps. First, one indicates in the given error vector a sequence of elements by randomly chosen start and end elements. Second, this string is moved to a randomly chosen position inside the error vector, or alternately, is simply reversed. With this new error vector, a new value of the objective function W is calculated. If the new distribution results in a smaller value of the objective function, it is taken as a new reference of error set. Also, in case the new objective function is larger and differs by an amount $W-W_0=\Delta W>0$, this distribution will be taken as the new reference, if $e^{-\Delta W/T}$ is above a given (randomly chosen) threshold. Here T serves as a temperature-like parameter, which is lowered with the increasing number of permutations. In this way one scans the values of the objective functions in the vicinity of the present reference point but avoids being trapped in a local minimum. This is known as the Metropolis algorithm [5]. The resulting solution of the objective functions is not necessarily the smallest one, but it is close to the minimum. The advantage of this algorithm is that it can escape from local minima and so more of the configuration space can be explored.

4 Sorting simulation results

The lattice at tune point (9.3, 5.2) and chromaticity (2, 2) has been assumed for the sorting of the placements of dipole, quadrupole and sextupole magnets based on their magnetic field data [9] for the Indus-2 storage ring. For the commissioning of any storage ring or synchrotron, the first step is to make the beam injection and one turn circulation of the beam. Keeping this in view, it has been decided to sort the placement of the magnets for the magnetic field errors at injection energy. For Indus-2, the expected injection energy is 0.60 GeV. Once the injection is completed and the beam is stored then the machine parameters can be measured and correction action can be taken.

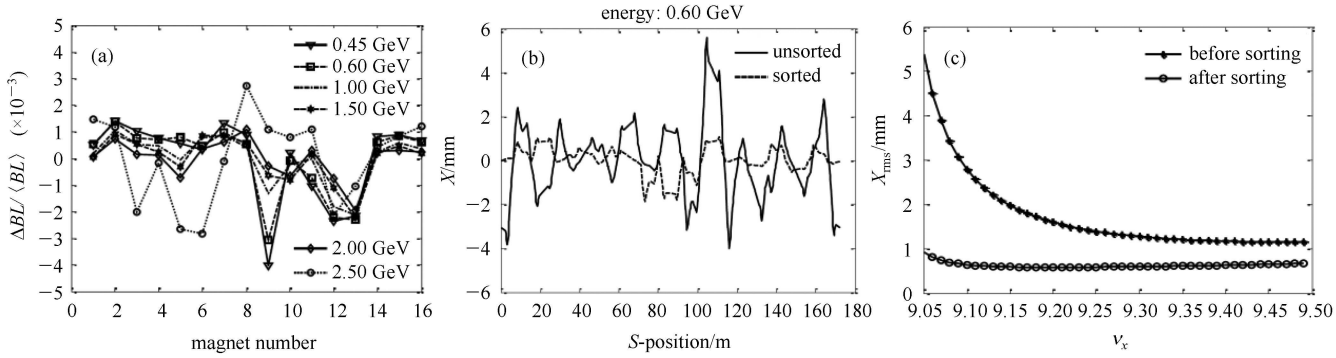

Fig. 2. (a) $\Delta BL/\langle BL\rangle$ in dipole magnets at various energy levels, (b) closed orbit distortion before and after sorting the dipoles at 0.6 GeV and (c) effect of sorting the dipole magnets on rms of closed orbit with different horizontal tunes at fixed vertical tune =5.2.

4.1 Dipole sorting

For the dipole sorting, no multipole effects and no effect of cavity are taken into the calculations. The measured rms dipole field strength errors at 0.45, 0.6, 1.0, 1.5, 2.0 and 2.5 GeV energies are 1.5×10^{-3}, 1.3×10^{-3}, 9.1×10^{-4}, 8.1×10^{-4}, 7.1×10^{-4} and 1.6×10^{-3} respectively and the distribution of the magnetic field errors are shown in Fig. 2(a).

An attempt has made to sort the dipole magnets with their field errors using a local compensation scheme. For the present lattice at the dipole centre, where the beta functions are the same and the phase advance between the centre-to-centre of the dipole magnets is 180°, the local compensation scheme works well. Out of 16 errors 10 are identified to make 5 pairs and the remaining 6 errors, which are very different in magnitude, are permuted and a minimum of W was searched. As the local compensation scheme may not be applicable for quadrupoles and sextupoles, sorting the dipole sorting has also been done by a simulated annealing algorithm. The optimized sequence obtained by simulated annealing gives more of an advantage over the local compensation scheme.

The effect of the sorted sequence of dipoles on the closed orbit over the ring is shown in Fig. 2(b). The effect on the maximum and RMS of the closed orbit over the entire ring before and after sorting, at various energies, are tabulated in Table 3. From Table 3 it can be seen that by placing the dipole magnets at optimized locations, the COD reduces in maximum and RMS by 65% and 63% compared to the unsorted situation. This sorted sequence is effective, i.e. there is always a reduction in the closed orbit, all along the energy range.

Keeping in view that the actual machine may be operating at a different tune point other than the design tune (9.3, 5.2), the effect of sorting on COD at different tunes are checked. The effect was seen by varying the horizontal tune and keeping the vertical tune fixed and the results are shown in Fig. 2(c). It shows that there is always a reduction in RMS closed orbit with the sorted dipole sequence with respect to unsorted COD at different horizontal tunes. We have also checked the effect of sorting at altogether different tune (9.3, 6.2), which is the present operating optics. The sorting of the dipoles reduce the RMS closed orbit at any scanned optics.

Table 3. Effect of dipole magnet sorting on closed orbit at various beam energy levels.

beam energy/	before sorting		after sorting	
GeV	max/mm	RMS/mm	max/mm	RMS/mm
0.45	6.18	2.10	2.43	0.84
0.60	5.43	1.60	1.88	0.58
1.00	2.55	0.95	2.86	1.09
1.50	3.53	1.16	3.16	1.15
2.00	3.03	0.99	3.07	0.92
2.50	6.46	2.30	4.90	1.73

4.2 Quadrupole sorting

After optimising and fixing the locations of the dipole magnets, the quadrupolar components in the dipoles, shown in Fig. 3(a), are also considered while sorting the quadrupole magnets. As each pair of the first three families of quadrupoles, i.e. Q1D, Q2F and Q3D, is driven by one power supply, the pairing of the quadrupole magnets was made. This pairing was done by searching the quadrupoles in pairs having magnetic fields closed to each other. In sorting, each pair was treated as a single parameter. In the Q3D family, due to geometry, out of 16 magnets, 8 which are 'open type' should be placed downstream of the dipoles and the remaining 8, which are 'closed type', should be placed upstream of the dipoles. The constraint due to geometry is also imposed on the Q4F family of quadrupoles as in Q3D. The quadrupoles in the Q4F family are driven by one power supply and are divided into two groups based on 'open type' and 'closed type' quadrupoles. Out of 16 quadrupoles, 8 odd

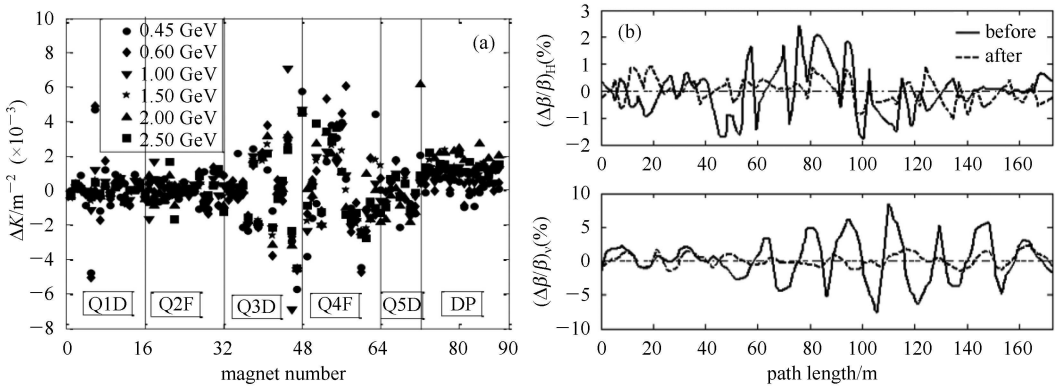

Fig. 3. (a) Normalized field errors in five families of quadrupoles and quadrupolar components in dipole magnets at various energy levels and (b) percentage of beta beat in horizontal and vertical planes before and after sorting the quadrupole magnets with their field errors.

numbers of quadrupoles from the point of injection are 'open type' and the other 8 are 'closed type'. Even though there are 16 magnet-to-magnet field errors, no quadrupole from one group can enter into the other group and while sorting the magnets, the rearrangements should be within the group. All 8 quadrupoles of the Q5D family are treated as independent parameters. The magnet-to-magnet gradient errors in the quadrupoles, as shown in Fig. 3(a), are used to calculate the objective function. After applying all the magnet-to-magnet gradient errors in the quadrupoles for their actual sequence, the tune also changes from its design value. There is a considerable change observed in the vertical tune and it is expected that beta beat in this plane will be larger.

Sorting has been carried out for all families of quadrupoles simultaneously with their field gradient errors. After optimizing the places of the quadrupoles, the minimum of the objective function is attained. The final objective function is reduced by one order of magnitude. The effect on beta beat over the ring before and after optimization in the horizontal and vertical planes is shown in Fig. 3(b). There is 57% and 67% reduction in maximum beta beat in the horizontal and vertical planes and 52% and 71% reduction in the RMS beta beat in the horizontal and vertical planes respectively. The effects of this sorted sequence, on maximum and RMS percentage of beta beat at various beam energy levels, are listed in Table 4. From Table 4 it can be observed that the optimized sequence obtained is effective at other beam energy levels. It is to be noticed that the quadrupole gradient errors led to a larger contribution to the beta beat in the vertical plane. The sorting algorithm is very effective in this plane and it reduces the beta beat with a larger gain.

Table 4. Effect of quadrupole sorting on percentage of beta beat at various beam energy levels.

beam energy/GeV		$\frac{\Delta\beta}{\beta_0}$%			
		unsorted		sorted	
		max	RMS	max	RMS
0.45	H	3.2	1.38	2.47	1.15
	V	6.71	2.52	3.53	1.13
0.60	H	2.42	0.89	1.05	0.43
	V	8.38	3.22	2.30	0.93
1.0	H	1.16	0.48	0.99	0.47
	V	6.78	2.75	4.44	1.72
1.5	H	0.99	0.43	0.87	0.29
	V	8.15	3.04	4.78	1.99
2.0	H	0.96	0.47	1.38	0.49
	V	11.93	4.46	9.76	3.43
2.5	H	1.47	0.66	1.43	0.55
	V	6.55	2.62	5.91	2.13

H & V: stand for horizontal and vertical planes.

The sextupolar components in the sorted sequence of dipole magnets are considered as shown in Fig. 4. The magnet-to-magnet field errors in the SF and SD family of sextupoles are also shown in Fig. 4. For the working tune point of (9.3, 5.2) the distortion functions are minimized and the effect on the dynamic aperture is seen by tracking the particle for a different number of turns. No gain in dynamic aperture is achieved in the presence of the main sextupoles. For various working tune points, sorting is done and no or little improvement in dynamic aperture is observed. So it was decided that the sorting of sextupole magnets is not required.

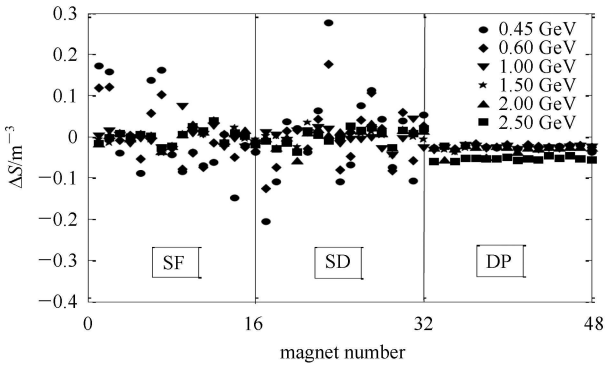

Fig. 4. Normalized sextupole to sextupole field errors and sextupolar components in dipole magnets at various energy levels.

Including quadrupolar and sextupolar components in dipoles and magnet-to-magnet field errors in dipoles and quadrupole families, dynamic aperture has been calculated using frequency map analysis [10] for unsorted and sorted sequences of the magnets. For comparison, a dynamic aperture has also been calculated with bare lattice, i.e. without any field errors. For the bare lattice in the presence of chromaticity correcting sextupoles the dynamic aperture is more than 35 mm in the horizontal and 17 mm in the vertical plane respectively. With the unsorted errors it was reduced to 24 mm and 15 mm in the horizontal and vertical planes. After sorting the magnets with their field errors the dynamic aperture recovered and improved to ∼30 mm and ∼16 mm in the horizontal and vertical planes. We have also seen the effect of sorting on the beam emittance. Before sorting the beam emittance increased to 67.9 nm·rad from the ideal value of 58 nm·rad. After sorting the beam emittance was recovered to the value of 60 nm·rad. The magnetic elements were placed in the ring as per their optimized positions in the Indus-2 storage ring. In Indus-2, the electron beam circulated for a few turns without the injection kicker magnets and later on the beam was accumulated with the RF cavity turned on at the injection energy. This was achieved without energizing any of the corrector magnets. The sorted sequence of the magnetic element resulted in sufficient available beam aperture.

5 Measured results

After placing the magnets at an optimized location real beam commissioning was started. The electron beam circulated first one turn and then four turns without injection kickers with ease. With injection kickers turned on beam circulation lasted for ∼2.5 ms (1 turn is equal to ∼575 ns revolution time) and later with RF cavity turned on the storage of the electron beam without energizing any of the steering magnets has been achieved. Presently Indus-2 is being operated at injection energy 0.55 GeV for beam accumulation and full energy of 2.5 GeV with 100 mA beam current in user mode.

After successful accumulation of the beam current the measurement of various parameters was started. We report here the measurement of COD, beta beat, dynamic aperture and the effect on beam accumulation rates before and after COD correction. In the real machine the contribution to COD will also come from the alignment errors of the quadrupoles which we have not considered in simulations. The resulting COD may be different than the simulated orbit obtained from the dipole magnet-to-magnet field errors. The measured horizontal and vertical COD at injection energy are shown in Fig. 5(a). Beam injection was taking place even without correcting the COD but with a poor beam injection rate. The horizontal COD at the injection point is negative which helps in the injection. With COD correction this becomes near to zero and brings the orbit nearer to the injection septum as the injection is taking place from the outside of the ring, and results in the difficulty of beam accumulation. The horizontal COD correction at injection energy was optimized using the constrained COD correction method [11] in such a way that there should be overall correction, but the COD at the injection point remained unchanged. There are two BPMs, namely LS1-BPM2 and LS1-BPM3, placed in the injection bump zone. As seen by the circle in Fig. 5(a), the horizontal orbit at these two BPMs is the same as before COD correction. It means the injection conditions, i.e. the injection kicker settings, can remain the same as the settings without COD correction. The RMS after horizontal COD correction is 1.65 mm while uncorrected was 4.5 mm. The uncorrected and corrected vertical COD are shown in Fig. 5(b). The vertical RMS COD is 0.7 mm while uncorrected was 1.7 mm. The COD correction was made so that any of the steering magnet strengths should not get saturated up to 2.5 GeV operation in user mode.

A beam accumulation rate comparison up to 100 mA beam current accumulation with and without COD correction is shown in Fig. 6. Normally the injection without COD correction is taking place. In the typical beam injection the injection rate is about 36 μA/s. After applying the COD correction the injection rate improves to 55 μA/s. During this experiment the booster current was ∼2.5 mA. The injection kickers and timing setting were kept the same as the bump amplitude and should remain the same even with COD correction. With the increase of booster current up to 4 mA, the beam accumulation rates in Indus-2 also increased to ∼90 μA/s.

We have also measured the average beta functions at quadrupole locations in both the horizontal and vertical planes by conventional quadrupole scan method [11] and

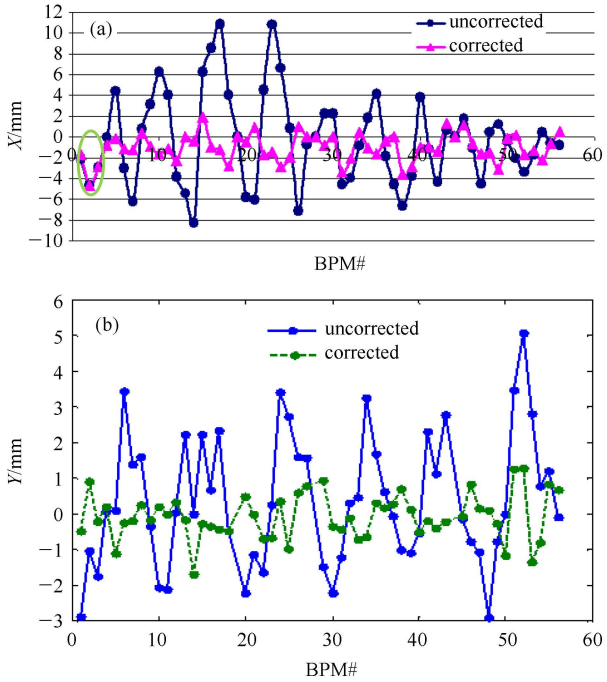

Fig. 5. (a) The uncorrected and corrected horizontal COD at injection energy. The horizontal orbit at the injection zone is the same with and without COD correction as shown in the circle; (b) The uncorrected and corrected vertical COD at injection energy.

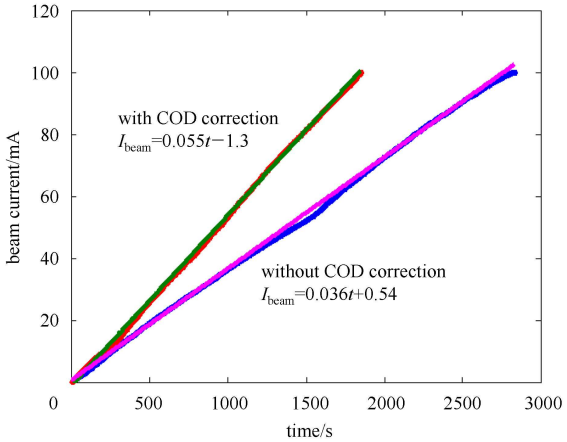

Fig. 6. The comparison of beam accumulation rates with and without COD correction.

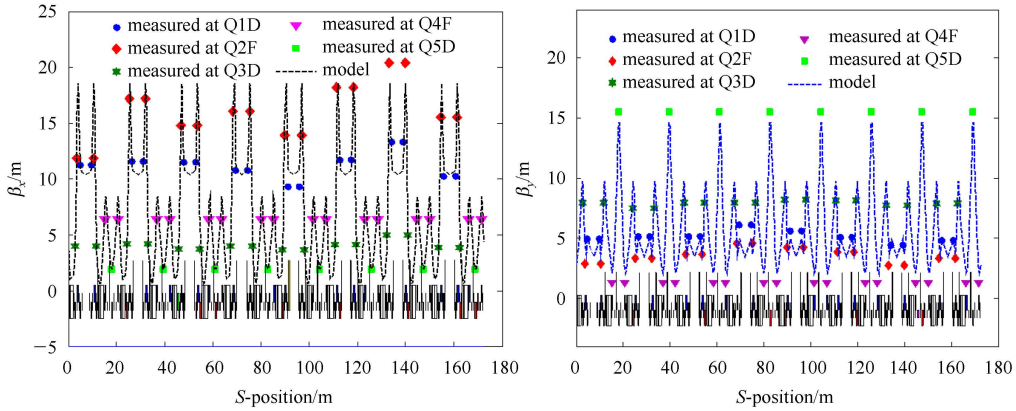

Fig. 7. The model and measured horizontal average beta functions at quadrupole locations obtained by quadrupole scan method in horizontal and vertical planes.

the results are shown in Fig. 7. The measured beta beat is ∼15%–20% in both the planes. The measured beta beat is higher than the beta beat obtained by sorting the quadrupoles. This may be due to the calibration error of the quadrupole power supplies. The measured dynamic aperture in one of the eight long straight sections at the corrected COD is > 20 mm in the horizontal and >8 mm in the vertical plane.

In this paper we have reported only the measured parameters relating to the sorting of the dipoles, quadrupoles and sextupoles at the injection energy. A comprehensive list of the measurement and analysis of parameters in Indus-2 at the injection energy as well as at intermediate energy 2 GeV and final energy 2.5 GeV have been reported recently in Ref. [12–14].

6 Conclusions

The simulated annealing algorithm used to obtain the optimal placement of the magnets depending on their field strength errors in the Indus-2 ring is quite effective. The dipole and quadrupole magnets are placed in the ring according to the optimized locations in the ring. By the optimization of dipole placement, closed orbit distortion is reduced by a factor of three in RMS and maximum value over the ring. The percentage of beta beat in the vertical plane due to the sorted sequence of quadrupoles is also reduced by a factor of three with respect to the un-optimized sequence. The effect of sextupole sorting is insignificant when chromaticity correcting sextupoles are included, since the dynamic aperture is dominated by the main sextupole component. Therefore, sorting the main chromaticity correcting sextupole magnets was not recommended. By sorting, the dynamic aperture has improved by ∼6 mm in the horizontal and 1 mm in the vertical planes. The magnets are placed in the ring with the optimized sequence, and storage of the beam has been achieved at injection energy without energizing any steering magnets. With the stored beam current various parameters were measured and with COD correction the injection efficiency has improved by nearly a factor of 2.

We thank the colleagues of the Indus-2 operation team at the Indus accelerator complex for their help in taking the measurements. One of the authors (GS) is thankful to the Department of Atomic Energy for the award of Raja Ramanna Fellowship.

References

1 Kotaiah S et al. Present Status of Synchrotron Radiation Source Indus-2. Indian Particle Accelerator Conference, 2005. 1
2 Abo-Bakr M, Wustfeld G. Sorting of Magnets for the BESSY-Ⅱ Booster and Storage Ring, European Particle Accelerator Conference, 1996. 1341
3 Salamon P, Sibani P, Frost R. Facts, Conjectures and Improvements for Simulated Annealing, SIAM Society of Industrial & Applied Mathematics, Philadelphia, PA. 2002
4 Press W H et al. Numerical Recipes in C. 2nd Edition. Cambridge UK: Cambridge University Press, 1992
5 Kirkpatrick S. Journal of Statistical Physics, 1984, **34**: 975
6 Montague B W. Chromatic Effects and Their First Order Correction, CERN 87-03, Geneva, 1987
7 Dinev D. Nucl. Instrum. Methods Phys. A, 1996, **381**: 209
8 Bengtsson J. The Sextupole Scheme for Swiss Light Source (SLS): An Analytical Approach, SLS Note 9/97
9 Sinha G et al. Magnetic Field Measurements for Indus-2 Magnets, Private Communication
10 Nadolski L, Laskar J. Phys. Rev. ST Accel. Beams, 2003, **6**: 114801
11 Harada K et al. Nucl. Instr. Methods Phys. Research A, 2009, **604**: 481–488; http://dx.doi.org/10.1016/j.nima.2009.03.238
12 Ghodke A D et al. Rev. Sci. Instrum., 2012, **83**: 103303; http://dx.doi.org/10.1063/1.4760254
13 Riyasat H et al. Pramana–J. Phys., 2013, **80**(2): 263; 10.1007/s12043-012-0482-3
14 Kumar P et al. Rev. Sci. Instrum., 2013, **84**: 123301; http://dx.doi.org/10.1063/1.4833395